LANGMUIR

pubs.acs.org/Langmuir Article

Where Are Sodium Ions in AOT Reverse Micelles? Fluoride Anion Probes Nanoconfined Ions by ¹⁹F Nuclear Magnetic Resonance Spectroscopy

Samantha L. Miller, Ernestas Gaidamauskas, Ataf Ali Altaf, Debbie C. Crans, and Nancy E. Levinger



Cite This: Langmuir 2023, 39, 7811-7819



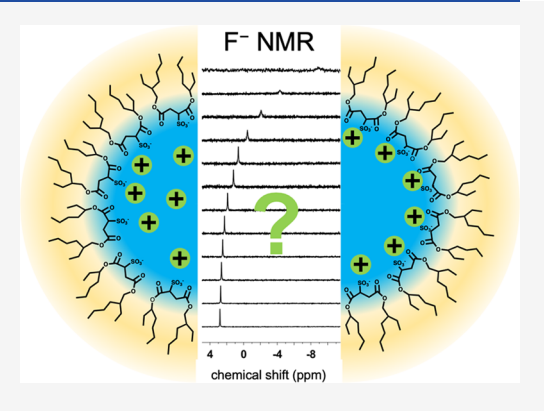
ACCESS I

III Metrics & More

Article Recommendations

Supporting Information

ABSTRACT: Confining water to nanosized spaces creates a unique environment that can change water's structural and dynamic properties. When ions are present in these nanoscopic spaces, the limited number of water molecules and short screening length can dramatically affect how ions are distributed compared to the homogeneous distribution assumed in bulk aqueous solution. Here, we demonstrate that the chemical shift observed in ¹⁹F NMR spectroscopy of fluoride anion, F⁻, probes the location of sodium ions, Na⁺, confined in reverse micelles prepared from AOT (sodium dioctyl sulfosuccinate) surfactants. Our measurements show that the nanoconfined environment of reverse micelles can lead to extremely high apparent ion concentrations and ionic strength, beyond the limit in bulk aqueous solutions. Most notably, the ¹⁹F NMR chemical shift trends we observe for F⁻ in the reverse micelles indicate that the AOT sodium counterions remain at or near the interior interface between surfactant and water, thus providing the first experimental support for this hypothesis.



■ INTRODUCTION

Nanoconfined aqueous solutions exist in a wide range of samples from biological systems such as cells and organelles, in channels and minuscule pockets in proteins, to pores in minerals and metal oxides, and in a wide range of synthetic materials. The properties of homogeneous aqueous solutions can be drastically affected when those solutions are confined to droplets on the nanometer scale. When aqueous solutions are restricted in size, the presence and location of ions in these aqueous solutions can also play a strong role in the properties of any system and can mediate its chemistry. 1–6

Reverse micelle structures present a common and easily tuned system demonstrating the role of nanoconfinement on the chemical and physical properties of encapsulated ions. ^{7–9} Reverse micelles are self-assembled droplets of polar solvent stabilized in nonpolar solvent by an amphiphile, whose cartoon representation as we often represent them appears in Figure 1. The reverse micelle size is conveniently controlled by adjusting the ratio of water to surfactant in solution, given by $w_0 = [H_2O]/[surfactant]$. Assuming a spherical shape, w_0 is directly proportional to the average radius of the reverse micelle. ¹⁰ Although we often assume that reverse micelles are largely spherical, all-atom simulations ^{11–18} and a few experimental studies ^{15,19–21} demonstrate that they are only spherical on average, instantaneously exhibiting a range of irregular, nonspherical shapes. ^{11–18,22} Still, it is clear that larger w_0 results in a larger average reverse micelle hydrodynamic radius. ¹⁰ Nearly all papers published about reverse micelles

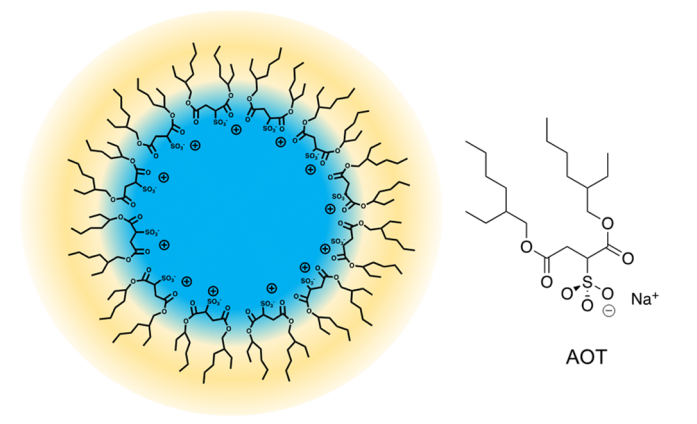


Figure 1. Cartoon depiction of an AOT reverse micelle and molecular structures of AOT surfactant. The blue interior represents the nanosized water droplet, yellow indicates the nonpolar solvent isooctane, and circles represent the sodium cations associated with the AOT headgroup.

Received: March 8, 2023 Revised: May 9, 2023 Published: May 23, 2023





include a cartoon like the spherical structure shown in Figure 1, where surfactant counterions are neatly paired to the surfactant molecule. All-atom simulations indicate that the surfactant counterions remain largely at the interior interface 11-18 but no experimental results confirm the position of the counterions.

In bulk aqueous solution, soluble salts are considered to disperse uniformly in aqueous solution. The salt concentration can be conveniently controlled, and the resulting concentration can be experimentally confirmed using electrochemical methods. In a nanoconfined system created with ionic surfactants, it is unclear how to consider the contribution of surfactant counterion to the intramicellar solution. Both simulations¹¹⁻¹⁸ and experiments^{7,8} suggest that reverse micelles include a surfactant boundary layer with strongly bound water and counterions, and a more bulk-like core of water at the center. Chowdhary and Ladanyi showed that away from the interface, water reached a bulk-like density.1 Likewise, steady-state and time-resolved IR studies observe a population of bulk-like water that develops with increasing size, which would suggest that surfactant counterions reside at the interface. Experiments probing intramicellar pH have shown evidence for neutral water in the center of reverse micelle that suggests that the interface has extremely dynamic pH. This also suggests that there is a propensity for the surfactant counterions to migrate to the interface. 7,23-Simulations by both Abel et al. 11 as well as Mudzhikova and Brodskaya¹² and Chowdhary and Ladanyi all show that the AOT sulfur atom always has at least one sodium cation as a nearest neighbor.

So how can one measure the arrangement of ions in nanoconfined, heterogeneous spaces? With a 1/2 nuclear spin, 100% abundance of the ¹⁹F isotope, and resonant frequency close to the ¹H NMR resonance, ²⁸ fluorine is a very convenient nucleus and is routinely used for the characterization of Fcontaining compounds. 29-33 Several features make 19F NMR of the fluoride ion, F-, suitable as an environmental probe. Fluorine's chemical shift range is 25-fold larger than the proton giving greater response to local magnetic field compared to hydrogen making it sensitive to environmental changes. 32,34,35 The fluoride anion is sensitive to its environment and thus an excellent reporter for changes in its environment. Indeed, a range of studies have documented the effects of solvents, pH, and the presence of solutes on the fluoride NMR signal. 32,34–38 Fluoride is also sensitive to the ionic strength of the solution, making it a potential nanoconfinement-compatible probe of ions in confinement. ^{39,40} Finally, fluoride interacts strongly with H2O, so it senses effects on aqueous environments rather than partitioning to interfaces in reverse micelles. Due to its strong interaction with water and expected Coulombic repulsion from surfactant headgroups, we anticipate fluoride will reside largely in the interior water pool.

Here, we demonstrate that ¹⁹F NMR of F⁻ can serve as a measure of the nanoconfined environments of reverse micelles in situ. Comparison of the ¹⁹F NMR chemical shift arising from F⁻ in bulk aqueous solutions provides a framework for sodium cation concentration and can serve as a guide to interpret signals measured for F⁻ in AOT reverse micelles. We use results from bulk aqueous solution and an estimation of what the sodium cation concentration would be inside the reverse micelles to show that the ions are not uniformly distributed but rather largely associated with the reverse micelle inner surface.

MATERIALS AND METHODS

Materials. Reagent-grade NaF, NaNO₃, NaBr, Na₂SO₄, and isooctane (2,2,4-trimethylpentane) were purchased from Sigma-Aldrich Chemical Co. and used without further purification. AOT (sodium dioctyl sulfosuccinate, Sigma-Aldrich Chemical Co.) was purified to remove an acidic contaminant as described previously. Deuterium oxide (D₂O, Cambridge Isotope Laboratories, 99.9%), NaOD (Merck & Co., 98 atom % D), cyclohexane (Aldrich, anhydrous, 99.5%), and DCl (Sigma-Aldrich, 99.5 atom % D) were used as received. Deionized water (18 MΩ·cm) was used to prepare all aqueous solutions using a commercial filtration system (Fisher Scientific, Milli-Q).

Stock Solutions and Sample Preparation. Stock solutions of sodium fluoride (NaF) in H_2O (or in D_2O) were prepared at the indicated salt concentration. To prepare concentrated stock solutions of NaNO₃, NaBr, and Na₂SO₄, solutions were heated until the solids completely dissolved. After cooling to ambient temperature, solutions were further diluted with H_2O or D_2O to the desired F^- and salt concentration (100 or 25 mM). We measured solution pH (Corning 140 pH meter equipped with a combination microelectrode), adjusting for pD using the formula pD = pH + 0.4.⁴² Sample pH/pD was adjusted to 6.9, well separated from the pK_a value for HF of 3.2,⁴³ to ensure that all fluorine in the samples was in the form of F^- rather than HF (see Figure S2). To prepare the stock solution with acidic pH, we added HCl or DCl and measured pH/pD until it remained constant at ambient temperature (300 \pm 1 K).

Reverse Micelle Solutions. The 0.20 M AOT stock solution was prepared in 2,2,4-trimethylpentane (isooctane). The reverse micelle solutions were prepared in glass vials by mixing the appropriate volume of 0.20 M NaF aqueous solution (pH 6.9) and respective surfactant stock solutions. The size of reverse micelles, w_0 , was controlled by the ratio of 0.20 M NaF aqueous solution to the surfactant solution in isooctane. After mixing, the samples were vortexed in closed vials until clear solutions were obtained, ensuring the formation of reverse micelles. If phase separation occurred, the samples were gently warmed until a single clear phase was observed and cooled back to room temperature. Only clear and nonopalescent solutions were used for NMR spectroscopy and dynamic light scattering (DLS).

NMR Spectroscopy. The ^{19}F NMR spectra were acquired at 25.0 $^{\circ}C$ using a Varian Inova 300 spectrometer operating at 282.20 MHz, using the unlocked mode settings without 2H lock, as reported previously for these complex samples. 41 A standard pulse sequence was used with 0.5 s relaxation delay, 10° pulse width, and 0.3 s acquisition time. All ^{19}F chemical shifts are referenced by substitution against the external 0.01 M NaF solution in D₂O (pH 12.0) without frequency lock. The reproducibility of the chemical shift was ± 0.1 ppm; spectra for each experimental condition were collected in triplicate to ensure reproducibility.

Aqueous 1 H NMR samples were recorded on Varian Inova 300 spectrometer operating at 299.95 MHz. Chemical shifts were referenced against external DSS (sodium 4,4-dimethyl-4-silapentane-1-sulfonate) in $\rm D_2O$ ($\delta_{\rm DSS}=0.00$ ppm). The AOT/isooctane/HOD samples were referenced against isooctane signals 0.905 (Me, s), 0.922 (Me, d), 1.146 (CH₂, d), and 1.676 ppm (CH, m). The chemical shift reproducibility was within 0.002 ppm. Spectral data were processed using MNova. Although the experiments described here are relatively straightforward to set up and perform, precision in sample preparation as well as strong attention to the details of samples and experimental conditions, e.g., pH, temperature, and pressure (exposure to carbon dioxide), is necessary to ensure accurate and reproducible results.

Dynamic Light Scattering (DLS). DLS (Malvern Zetasizer ZS, model ZEN3600) measurements were performed on the reverse micelle samples containing F⁻ and the corresponding control samples containing only deionized water. Prior to data acquisition, the samples were equilibrated in the DLS instrument for 90 s at 25 °C. Scans were averaged from 30 scans in backscatter mode (173°).

RESULTS AND DISCUSSION

¹⁹F NMR as a Probe of Ionic Strength: Aqueous Ionic Solutions. Before using ¹⁹F NMR of F⁻ to measure the concentration of sodium ions in nanoconfined environments, we prepared and measured a series of bulk aqueous NaF solutions of known ionic strength. Figure 2 shows the ¹⁹F

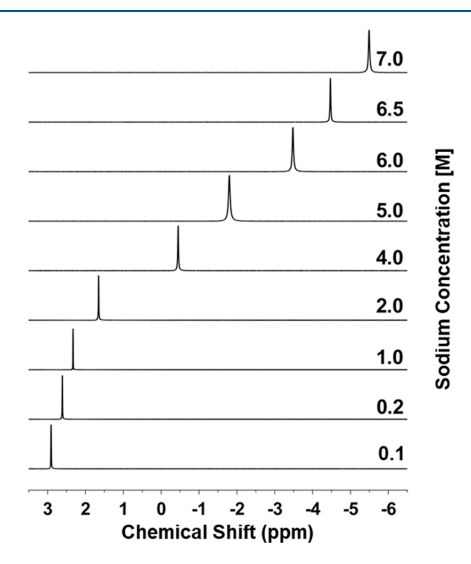


Figure 2. Representative ^{19}F NMR spectra of fluoride in bulk aqueous NaNO3 solution as a function of increasing ionic strength. Numbers on the right-hand side indicate sodium ion concentration based on [NaNO3]. Spectra were acquired at 25 $^{\circ}C$, and all solutions were prepared to pH = 6.9 \pm 0.1. Chemical shifts of the F^- peak are referenced by substitution against the 0.01 M NaF in D2O (pH 12.0) without lock.

NMR spectra for F⁻ in this series of bulk aqueous solutions. At the lowest concentration measured, 0.01 M NaF, the F⁻ displays a chemical shift of 2.9 ppm. All other solutions that we measured were prepared with 0.2 M NaF with increasing NaNO₃ to change the sodium ion concentration. As we increase the ionic strength of the aqueous solution, the F⁻ peak shifts upfield toward smaller values, which indicates greater shielding of the fluoride ion. ^{44,45} At 7.0 M, the highest sodium ion concentration that we could attain using NaNO₃, the F⁻ peak appears at -5.5 ppm, representing an overall change of more than 8 ppm over the ionic strength range measured and shown in Figure 2.

We explored how the counter anion in different salts affects the response of F⁻ chemical shift as a probe of sodium ion concentration. Figure 3 depicts the F⁻ chemical shift measured as a function of sodium ion concentration obtained by adding various salts including NaBr, NaNO₃, and Na₂SO₄. As shown in Figure 3, changing the anion from nitrate to bromide or sulfate (accounting for divalency) has no impact on the F⁻ chemical shift; the ¹⁹F NMR chemical shift depends only on the sodium ion concentration. These data demonstrate that the ¹⁹F NMR chemical shift of F⁻ in these bulk aqueous solutions tracks the sodium ion concentration.

¹⁹F NMR of F⁻ in AOT/Isooctane Reverse Micelles. When we introduce F⁻ to the AOT reverse micelles, we also observe a shift in the ¹⁹F NMR peak position; Figure 4 shows the NMR spectra, and Figure 5 shows the chemical shift as a function of w_0 . Generally, as the w_0 value decreases, the chemical shift also decreases. From $w_0 = 20$ to 10, the chemical shift remains relatively constant, reaching an asymptote close

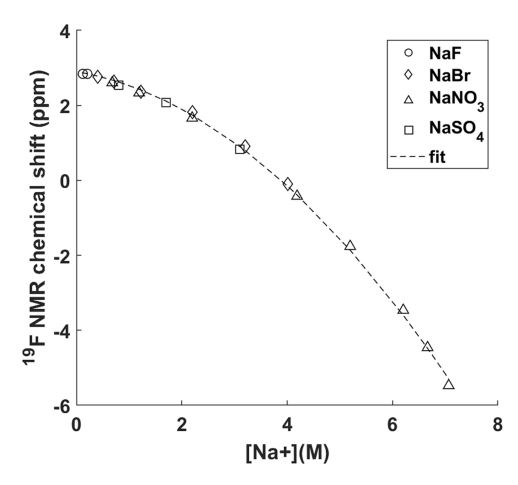


Figure 3. ¹⁹F NMR chemical shift as a function of sodium ion concentration in aqueous solutions of NaF (\bigcirc), and NaF binary mixtures with NaBr (\lozenge), NaNO₃ (\triangle), and Na₂SO₄ (\square) and fit to second-order polynomial (\cdots) given by δ = 2.9–0.173 [Na⁺] – 0.1457 [Na⁺]². This fit yields R^2 = 0.9969. The F⁻ concentration in binary salt mixtures was 0.20 M, and the solution pH was 6.8 \pm 0.3.

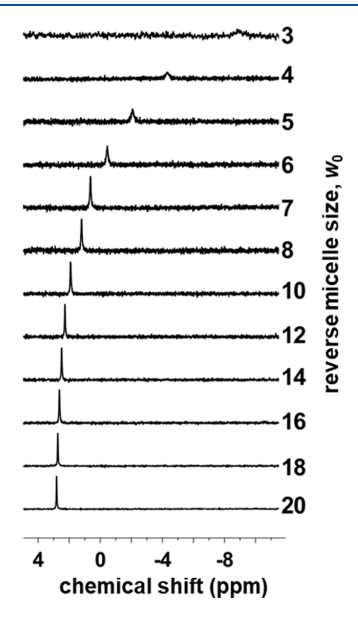


Figure 4. Representative ¹⁹F NMR spectra of F⁻ in AOT reverse micellar solutions with $w_0 = 3-20$ (labeled on the right of the spectra). Samples were prepared volumetrically from aqueous 0.20 M NaF solution (pH 6.9) and 0.20 M AOT in isooctane. All spectra were acquired at 25 °C. Chemical shift is referenced against the 0.01 M NaF in D₂O (pH 12.0) without lock.

to 3 ppm. As the reverse micelle size decreases below $w_0 = 10$, the F⁻ peak rapidly shifts to about -9.4 ppm for $w_0 = 3$, the smallest reverse micelle measured. This chemical shift value for the smallest reverse micelles appears at a significantly more negative value than -5.5 ppm, that is, the shift for the most concentrated bulk aqueous ionic solutions we measured at 7.0 M. In addition to chemical shift, we evaluated the width of the peaks in the ¹⁹F NMR spectra (see SI Figure S1). Over the w_0 range of 10-20, the linewidth does not vary and is approximately the same as in bulk aqueous solution. The linewidth increases sharply for smaller reverse micelles; the linewidth for the smallest reverse micelle measured, $w_0 = 3$ is approx. 10 times larger than the bulk aqueous solution or reverse micelles with $w_0 \ge 10$.

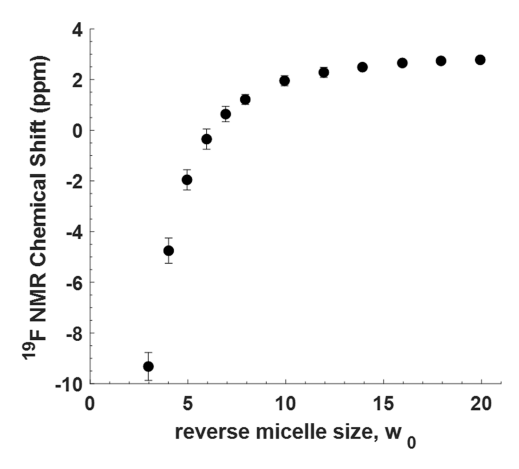


Figure 5. ¹⁹F NMR chemical shift of F⁻ in AOT reverse micelles vs w_0 . Error bars indicate standard deviations of three measurements.

 1 H NMR of Aqueous and AOT Reverse Micelle Solutions. We further characterized bulk aqueous ($D_{2}O$) and AOT reverse micelle samples using 1 H NMR spectroscopy to gauge the nature of the intramicellar water in reverse micelles prepared with 0.2 M NaF. Figure 6 displays the

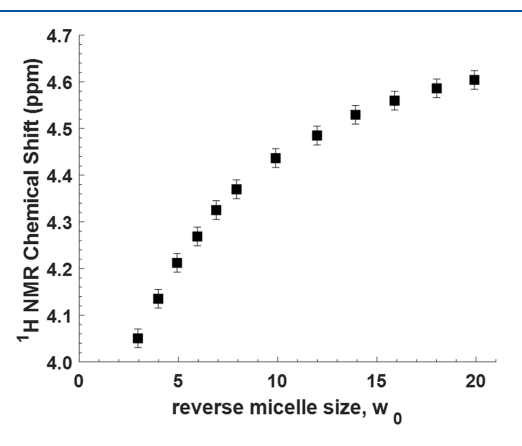


Figure 6. HOD chemical shift as a function of w_0 in AOT reverse micelles prepared with 0.20 M NaF. Samples were prepared from aqueous 0.20 M NaF solution (pH 6.9) and 0.20 M AOT solution in isooctane and measured at 25.0 °C. Error bars indicate standard deviations of three measurements.

chemical shift for HOD as a function of w_0 . The chemical shifts associated with ¹H in smaller reverse micelles appear upfield compared to those for larger reverse micelles. These results agree well with literature reports for bulk aqueous solutions that show the water peak shifts upfield with increasing sodium ion concentration. ⁴⁶

Effect of Fluoride Probe on AOT Reverse Micelle Size. Because preparing reverse micelles with solutions of high ionic strength has been demonstrated to affect reverse micelle particle size, $^{47-49}$ we used DLS to measure the AOT reverse micelle particle sizes prepared with water and with 0.2 M NaF, shown in Figure 7. The presence of F⁻ results in smaller reverse micelles compared to those prepared with pure water. At $w_0 = 10$, the size of the reverse micelles appears to plateau as a function of w_0 rather than continuing to grow like those containing water. The size difference we observe is similar to observations when other salts are added to AOT reverse micelles.

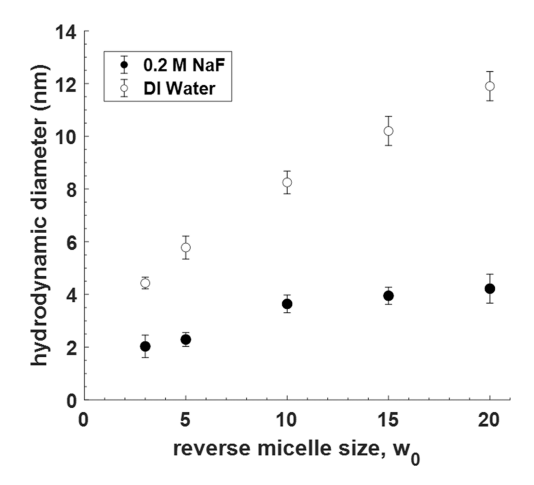


Figure 7. Hydrodynamic diameter of AOT reverse micelles as a function of w_0 . Reverse micelle solutions were prepared from deionized water (\bigcirc) , and aqueous 0.20 M NaF aqueous solution (\bullet) . Error bars indicate standard deviations of three measurements.

DISCUSSION

The chemical shift trends in our ¹⁹F NMR spectra of F-indicate that the AOT sodium counterions remain at or near the interior interface between the AOT surfactant and water. These measurements represent the first direct experimental evidence demonstrating the location of the sodium counterions in this nanoconfined space. The results also confirm predictions from all-atom and coarse grain simulations of AOT reverse micelles. ^{11–18}

In the larger reverse micelles we measured, the fluoride chemical shifts are similar to the shifts measured at lower sodium ion concentrations in bulk aqueous solution. For example, the measured ¹⁹F NMR chemical shift from fluoride is 2.80 ppm in 0.40 M NaBr and 2.77 ppm in a $w_0 = 20$ reverse micelle. Using the fit in Figure 3, we predict a sodium cation concentration of 0.44 M inside the reverse micelle even though the $w_0 = 20$ reverse micelle contains only 20 water molecules per sodium ion.

To compare the chemical shift trends from bulk aqueous solution with reverse micelles, we calculate a rough estimate of the intramicellar sodium ion concentration if all of the sodium counterions were distributed "uniformly" throughout the reverse micelle water pool (see the SI for a more detailed explanation of this estimation). The w_0 value provides the starting point of one sodium ion per volume occupied by water and sodium. We use the molar volume of water, 55.5 M, to estimate the volume associated with water molecules and the radius of the hydrated sodium ion computed in quantum simulations⁵⁰ to determine the sodium ion volume. From this, we generate an estimation of the sodium ion concentration by

$$[\mathrm{Na}^{+}] = \frac{1 \text{ mol Na}^{+}}{V_{\mathrm{molar}}(\mathrm{Na}^{+}) + w_{0} \cdot V_{\mathrm{molar}}(\mathrm{H}_{2}\mathrm{O})}$$
(1)

Using eq 1 and the fit to data in Figure 3, we predict the expected chemical shifts that solutions with these concentrations should produce (Table S1). Figure 8 shows a linear relationship between these predicted chemical shifts with the chemical shifts we measure from the reverse micelles; clearly, the experimentally measured chemical shifts are significantly less dramatic than those projected by our concentration estimation. The ¹⁹F NMR spectroscopy demonstrates that the

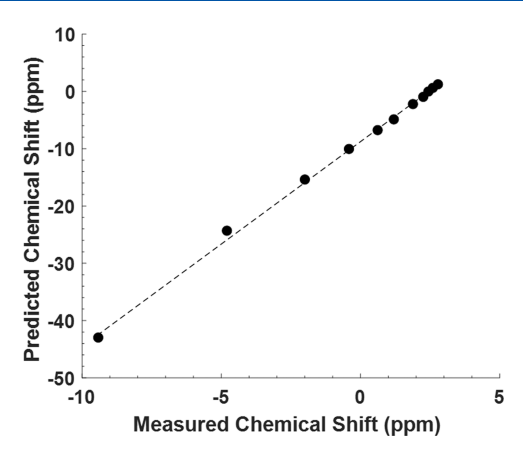


Figure 8. ¹⁹F NMR chemical shift predicted from w_0 values as a function of measured chemical shift for fluoride in AOT reverse micelles. Points represent data collected; line is the linear fit.

AOT aqueous interior has a significantly lower sodium ion concentration than the estimated concentration of sodium ions in the reverse micelles. This provides strong evidence indicating that the sodium cations are not distributed within the reverse micelle but rather remain near the sulfonate headgroups at the interface.

At least two factors likely cause surfactant counterions to reside largely at the interface: Coulombic attraction of counterions with the sulfonate headgroup and the inability of the water to screen charges from multiple cations within the water core. This insufficient screening can be interpreted in terms of the Debye screening length, which describes how far the electrostatic effect of a charge persists in solution. The Debye length is typically given by eq 2

$$\kappa^{-1} = \sqrt{\frac{\varepsilon_0 \varepsilon_r k_B T}{2N_A e^2 I}} \tag{2}$$

where ε_0 is the permittivity of free space, $\varepsilon_{\rm r}$ is the dielectric constant, $k_{\rm B}$ is the Boltzmann constant, T is the temperature (K), $N_{\rm A}$ is Avogadro's number, e is the elementary charge, and I is the ionic strength of the solution. A short Debye distance means that the electrostatic effect of ions does not extend far into the solution while a larger Debye distance means that an ion's effects are felt farther away from the ion in solution. For reference, the Debye length in a 1.0 M aqueous solution is approx. 0.3 nm, ⁵² meaning that the interior water pool of the reverse micelle has a similar dimension to the screening length. ¹⁰

Coulombic attraction between the water and the AOT sulfonate moiety could permit the water in the reverse micelles to screen the charges of the many sodium ions from the fluoride ions, therefore leading to the observed ¹⁹F NMR chemical shifts. This can only occur if the water pool in the AOT reverse micelles is sufficient to screen the fluoride ion from the sodium counterions inside the reverse micelles. From our DLS measurements (Figure 7), the hydrodynamic diameter of the $w_0 > 10$ reverse micelles is 3.8 nm, which translates to a water pool radius of \sim 0.5 nm, assuming the surfactant thickness is 1.4 nm. ¹⁸ In the 0.2 M NaF solution used to prepare the reverse micelles, the calculated Debye length is \sim 0.7 nm. To achieve sufficient screening, the F anion should be at least one Debye length from the cations, so the fluoride must reside at or near the center of the reverse

micelle water pool with the sodium ions residing at or near the interface.

With decreasing reverse micelle size, that is decreasing w_0 , the apparent sodium ion concentration inside the micelles should rise significantly. For $w_0 < 10$ AOT reverse micelles, the ¹⁹F NMR chemical shifts for intramicellar F⁻ change dramatically but still change much less than the concentration we predict from the relative sodium ion-to-water ratio as demonstrated in Figure 8. For the smallest AOT reverse micelles, the fluoride ion 19F NMR chemical shift is higher than any bulk aqueous solution we measured, suggesting an exceptionally high sodium ion concentration, ~8.8 M, greater than the signals we measured for 7 M sodium ion in bulk aqueous solution. Still, this concentration is far lower than 18.4 M, which is the concentration we predict for an even distribution of ions in the reverse micellar water pool. This effect can be accounted for if the sodium cations remain bound to the interface, then we expect a less dramatic change in chemical shift as reverse micelle size changes and the F⁻ anion is shielded by a stable water pool. The linewidths of the fluoride ¹⁹F NMR peaks support the interpretation that sodium ions reside largely at the inner interface of the reverse micelles. Specifically, the linewidths measured for larger reverse micelles, $w_0 \ge 10$, are similar to those in bulk aqueous solution, but when the reverse micelle size decreases to an extent that the fluoride senses the sodium counterions, then the environment likely becomes more variable, leading to broader peaks.

Our results complement work previously presented in the literature. Piletic et al. reported that in $w_0 = 10$ reverse micelles, approximately half of the water interacts with the interface and the rest forms a bulk-like water core. Likewise, Crans, Levinger, and co-workers have demonstrated a "buffering" effect of AOT reverse micelles interiors, where the intramicellar "pH" appears closer to neutral than bulk aqueous solutions from which micelles were prepared. Determine these results suggest that as long as the interior water pool of these reverse micelles keeps sodium counterions at the interface, molecules outside the Debye radius experience an environment similar to bulk water.

Unlike the results for ¹⁹F NMR spectroscopy, those for ¹H NMR show that the water peak shifts continuously with increasing reverse micelle size, w_0 , and does not approach a plateau like the ¹⁹F NMR results (see Figures 5 and 6). At first glance, this trend may seem inconsistent with the results for F in the reverse micelles. However, the ¹H NMR signals reflect all of the water molecules in the reverse micelles, which sample environments ranging from interface to interior. In small reverse micelles, most of the water molecules reside near or at the interface among the sodium ions and sense a very high concentration of sodium ions. In larger reverse micelles, some water molecules reside further from the interface sampling a relatively lower concentration solution. Thus, we expect that the water ¹H NMR spectra will continue to shift as the fraction of water near the interface decreases. The vast array of individual environments that the molecules sense along with fast chemical exchange between water molecules means that we only observe the average rather than molecules in any specific environment.^{6,8,53}

In related studies, the presence of ions added to the reverse micelle interior has been shown to contract the reverse micelle size. ^{48,49} Graeve and co-workers have observed a reduction in the size of AOT reverse micelles upon addition of ionic compounds such as NH₄OH, Al(NO₃)₃, ZrOCl₂. ^{47–49} Starting

with the Gouy—Chapman model for electrolytes near a charged surface, they explained the observed contraction as an indication of a reduced surfactant area due to overlapping electric double layers. This explanation asserted that smaller electrolyte cations displaced sodium ions from the surfactant interface. Graeve and co-workers related changes in reverse micelle size with both cation concentration and hydrated anion radius. He is in the literature of reverse micelle images presented in the literature of reverse micelle images presented in the literature of surfactant interface as and our cartoon in Figure 1 show, then this would result in an ionic strength gradient that is high at the surfactant interface and lower in the reverse micelle interior.

Our data aligns with these previous findings, as the DLS measurements also show a contraction in the size of AOT reverse micelles when prepared with 0.2 M NaF instead of pure DI water (Figure 7). The larger the w_0 , the greater the size-depression effect. Assuming that this contraction arises only from decreasing surfactant area, as hypothesized by Graeve, 47,48 but does not affect the number of surfactant molecules comprising the reverse micelle (aggregation number), then we can estimate the average number of Fions and the associated Sodium counterions at each w_0 value for our AOT reverse micelles using information from the literature. We provide these estimates in Table 1. We assume

Table 1. Relative Numbers of AOT, Water, and F⁻ Per Reverse Micelle Calculated According to Equation 7-f in ref 18

w_0	$n_{\rm agg}^{a}$	$\#H_2O$	#NaF/RM	ratio H ₂ O/F ^{-b}
3	13	40	0.1	39
4	19	78	0.3	76
5	27	133	0.5	135
6	35	210	0.8	210
7	44	311	1.1	275
8	55	440	1.6	275
10	80	800	3	275
12	110	1320	5	275
14	145	2030	7	275
16	184	2940	11	275
18	228	4110	15	275
20	277	5540	20	275

 $^{a}n_{\rm agg} = {\rm aggregation}$ number or the number of AOT molecules per reverse micelle and is calculated as $n_{\rm AOT} = 36\pi \left(w_0 + \frac{3}{2}\right)^2 \left(\frac{\overline{v}^2}{{\rm area}_{\rm AOT}}^3\right) + n_{\rm AOT}^0$ from ref 18. b At 0.2 M NaF, the ratio of water to Na⁺ or F⁻ is calculated to be 275.

that reverse micelle aggregates do not carry a net charge, so each reverse micelle containing fluoride has an additional associated sodium counterion from the introduction of NaF. For $w_0 > 7$ AOT reverse micelles, a Poisson distribution predicts at least one F⁻ per reverse micelle. Table 1 shows that below $w_0 = 7$, the average number of fluoride, and its associated sodium ion per reverse micelle is less than one, implying that some reverse micelles contain a F⁻ anion and its associated sodium ion while others do not include these ions. Interestingly, although we predict that only half the $w_0 = 5$ AOT reverse micelles prepared with 0.2 M NaF solution encapsulate a F⁻ anion and its associated sodium ion, DLS measurements (Figure 7) show that the reverse micelles are smaller than those prepared with the same volume of pure

water. This suggests that reverse micelles with NaF are even smaller than measured because the size represents an average between the standard-sized water-containing AOT reverse micelles and smaller reverse micelles that contain extra ions. Alternatively, the size reduction could indicate a different perturbation to the system such as a drop in aggregation number.

The analysis presented here depends on an accurate report of F chemical shift. Because the ¹⁹F NMR signal of aqueous F is sensitive to many variables including temperature, pressure, etc., measurements were performed in triplicate and other experiments were performed to ensure these controllable variables remained constant over the duration of the experiments measured. Repeat experiments provided very similar results to the reported patterns. Protonation of F⁻ in the reverse micelle environment could affect the interpretation of results reported here. The response of the fluoride probe we describe here cannot be attributed to a protonation event wherein the acidic species HF forms. When HF is present in the solution, an additional peak appears in the ¹⁹F NMR spectrum, as shown in Figure S2. This peak reflects the slow exchange between F- and HF under the experimental conditions. The chemical shift of HF using 19 NMR spectroscopy is a thoroughly studied phenomenon^{27,36-38} and would result in an independent HF peak that would appear upfield at approximately -160 ppm in an ¹⁹F NMR spectrum as described by a similar study that investigated HF in solutions of high ionic strength (I = 3 and I = 6). Even in studies where the HF ¹⁹F NMR chemical shift was measured in lower ionic strength solutions (I = 1), the expected chemical shift of an HF peak would be approximately -164.4, as reported by Finney et al.55

The data reported here could also be interpreted in terms of ionic strength. Although the concept and measurement of other bulk properties in nanoconfinement have been reported, e.g., pH,^{7,24,25,56-61} similar studies of ionic strength in nanoconfined spaces have not. Ionic strength has a profound effect on chemical structure and reactivity in a wide variety of systems. Most scientists consider the conventional definition of ionic strength,^{69,70}

$$I = \frac{1}{2} \sum_{i} a_i z_i^2 \tag{3}$$

where a_i is the activity of the charged species, often approximated by concentration, and z_i is the charge of that species. Although this expression works well for aqueous solutions at low to moderate concentrations, it may not apply in the anisotropic, heterogeneous nanoconfined environments present in reverse micelles. Furthermore, the response of fluoride to various cations depends on the specific cation. For example, changes in the fluoride chemical shift differ significantly even among alkali cations. 39,71-73 Thus, the fluoride chemical shift may show subtle differences with changes in ionic strength as the sample changes, particularly in systems with more than one cationic species. Nonetheless, if we interpret the fluoride chemical shift measured here as a measure of ionic strength, then we demonstrate that the inner surface of the reverse micelle presents an exceedingly high ionic strength while hundreds of picometers deeper into the water pool of the reverse micelle, the ionic strength is substantially lower.

CONCLUSIONS

Confining aqueous solutions to the nanoscale can have dramatic effects on the ion content and location in solutions, challenging our ability to measure or gauge bulk properties that are difficult or impossible to determine using standard laboratory methods. Here, we show that the chemical shift of the fluoride ion measured by 19F NMR spectroscopy can provide a measurement of the location of surfactant counterions in the nanoscopic environment of reverse micelles. For decades, researchers have drawn pictures of AOT reverse micelles showing the hypothetical location and organization of the sodium counterions. Computational studies have demonstrated the propensity for ions to reside associated with the interface, either as contact or solvent-separated ion pairs but none have been accompanied by experimental evidence. Here, we present the first experimental demonstration that sodium ions reside near or at the inner interface in AOT reverse micelles. These results are consistent with a range of other measurements on AOT reverse micelles that find differences in the nature of water in interfacial and interior locations and its heterogeneous nature compared to the homogeneous nature of bulk aqueous solutions. $^{6-9,11-20,23-25,27,41,47,48,53}$

These measurements also indicate that the sodium ion concentration in a nanoconfined structure (like a water droplet) can far exceed the limits of the bulk aqueous solution. Nonuniform ionic strength in these minuscule spaces has significant implications for the characterization of a wide range of heterogeneous systems, especially in environments like Nafion membranes used for fuel cell applications, whose porous features are similar to our reverse micelles. We see significant application for this straightforward measurement of aqueous homogeneity or heterogeneity that will reveal details about the nature of ionic solutions in nanoconfinement.

ASSOCIATED CONTENT

Supporting Information

The Supporting Information is available free of charge at https://pubs.acs.org/doi/10.1021/acs.langmuir.3c00649.

Detailed description of estimations of sodium ion concentration for reverse micelles and used in Figure 8 (Figure S1); linewidths for ¹⁹F NMR of fluoride in AOT reverse micelles as a function of w_0 (Figure S2); and ¹⁹F NMR spectra of fluoride in bulk aqueous solution and in reverse micelles prepared under various pH conditions showing where the HF peak appears (PDF)

AUTHOR INFORMATION

Corresponding Authors

Debbie C. Crans — Department of Chemistry, Colorado State University, Fort Collins, Colorado 80523, United States; Cell and Molecular Biology Program, Colorado State University, Fort Collins, Colorado 80523, United States; orcid.org/0000-0001-7792-3450; Email: Debbie.Crans@ColoState.edu

Nancy E. Levinger — Department of Chemistry, Colorado State University, Fort Collins, Colorado 80523, United States; Department of Electrical and Computer Engineering, Colorado State University, Fort Collins, Colorado 80523, United States; orcid.org/0000-0001-9624-4867; Email: Nancy.Levinger@ColoState.edu

Authors

Samantha L. Miller – Department of Chemistry, Colorado State University, Fort Collins, Colorado 80523, United States Ernestas Gaidamauskas – Department of Chemistry, Colorado State University, Fort Collins, Colorado 80523, United States

Ataf Ali Altaf — Department of Chemistry, Colorado State University, Fort Collins, Colorado 80523, United States; Department of Chemistry, University of Okara, Okara 56300, Pakistan; orcid.org/0000-0001-8018-5890

Complete contact information is available at: https://pubs.acs.org/10.1021/acs.langmuir.3c00649

Author Contributions

[⊥]S.L.M. and E.G. contributed equally to this work.

Note

The authors declare no competing financial interest.

ACKNOWLEDGMENTS

The authors gratefully acknowledge financial support from NSF grants 0628260 and 1956323. A.A.A. thanks the Higher Education Commission Islamabad, Pakistan, for a fellowship. The authors support the land acknowledgment of their home institution, Colorado State University, which can be found in its entirety at https://landacknowledgment.colostate.edu/.

REFERENCES

- (1) Luo, Z.-X.; Xing, Y.-Z.; Ling, Y.-C.; Kleinhammes, A.; Wu, Y. Electroneutrality Breakdown and Specific Ion Effects in Nanoconfined Aqueous Electrolytes Observed by NMR. *Nat. Commun.* **2015**, *6*, No. 6358.
- (2) Zhou, K.; Xu, Z. Nanoconfinement-Enforced Ion Correlation and Nanofluidic Ion Machinery. *Nano Lett.* **2020**, *20*, 8392–8398.
- (3) Diao, Y.; Espinosa-Marzal, R. M. Molecular Insight into the Nanoconfined Calcite—Solution Interface. *Proc. Natl. Acad. Sci. U.S.A.* **2016**, *113*, 12047—12052.
- (4) Qian, Y.; Wen; Adcock, P. A.; Jiang, Z.; Hakim, N.; Saha, M. S.; Mukerjee, S. PtM/C Catalyst Prepared Using Reverse Micelle Method for Oxygen Reduction Reaction in PEM Fuel Cells. *J. Phys. Chem. C* **2008**, *112*, 1146–1157.
- (5) Piler, K.; Mahmud, A.; Benson, T. J. A Regression Analysis with Laboratory Validation for the Use of Reverse Micelles to Achieve Desired Nanosized Catalytically Active Sites. *Chem. Eng. Commun.* **2020**, 207, 537–548.
- (6) Miller, S. L.; Wiebenga-Sanford, B. P.; Rithner, C. D.; Levinger, N. E. Nanoconfinement Raises the Energy Barrier to Hydrogen Atom Exchange between Water and Glucose. *J. Phys. Chem. B* **2021**, *125*, 3364–3373.
- (7) Crans, D. C.; Levinger, N. E. The Conundrum of pH in Water Nanodroplets: Sensing pH in Reverse Micelle Water Pools. *Acc. Chem. Res.* **2012**, *45*, 1637–1645.
- (8) Piletic, I. R.; Moilanen, D. E.; Spry, D. B.; Levinger, N. E.; Fayer, M. D. Testing the Core/Shell Model of Nanoconfined Water in Reverse Micelles Using Linear and Nonlinear IR Spectroscopy. *J. Phys. Chem. A* **2006**, *110*, 4985–4999.
- (9) De, T. K.; Maitra, A. Solution Behaviour of Aerosol OT in Non-Polar Solvents. *Adv. Colloid Interface Sci.* **1995**, *59*, 95–193.
- (10) Zulauf, M.; Eicke, H. F. Inverted Micelles and Microemulsions in the Ternary System Water/Aerosol-OT/Isooctane as Studied by Photon Correlation Spectroscopy. *J. Phys. Chem. A* **1979**, 83, 480–486
- (11) Abel, S.; Sterpone, F.; Bandyopadhyay, S.; Marchi, M. Molecular Modeling and Simulations of AOT-Water Reverse Micelles in Isooctane: Structural and Dynamic Properties. *J. Phys. Chem. B* **2004**, *108*, 19458–19466.

- (12) Mudzhikova, G. V.; Brodskaya, E. N. Molecular Dynamics Simulation of Surfactant Microaggregates in the Apolar Medium of n-Octane. *Colloid J.* **2005**, *67*, 451–458.
- (13) Gardner, A.; Vasquez, V. R.; Clifton, A.; Graeve, O. A. Molecular Dynamics Analysis of the AOT/Water/Isooctane System: Effect of Simulation Time, Initial Configuration, and Model Salts. *Fluid Phase Equilib.* **2007**, 262, 264–270.
- (14) Chowdhary, J.; Ladanyi, B. M. Molecular Dynamics Simulation of Aerosol-OT Reverse Micelles. *J. Phys. Chem. B* **2009**, *113*, 15029–15039.
- (15) Vasquez, V. R.; Williams, B. C.; Graeve, O. A. Stability and Comparative Analysis of AOT/Water/Isooctane Reverse Micelle System Using Dynamic Light Scattering and Molecular Dynamics. *J. Phys. Chem. B* **2011**, *115*, 2979–2987.
- (16) Martinez, A. V.; Dominguez, L.; Malolepsza, E.; Moser, A.; Ziegler, Z.; Straub, J. E. Probing the Structure and Dynamics of Confined Water in AOT Reverse Micelles. *J. Phys. Chem. B* **2013**, *117*, 7345–7351.
- (17) Agazzi, F. M.; Correa, N. M.; Rodriguez, J. Molecular Dynamics Simulation of Water/BHDC Cationic Reverse Micelles. Structural Characterization, Dynamical Properties, and Influence of Solvent on Intermicellar Interactions. *Langmuir* **2014**, *30*, 9643–9653.
- (18) Eskici, G.; Axelsen, P. H. The Size of AOT Reverse Micelles. *J. Phys. Chem. B* **2016**, *120*, 11337–11347.
- (19) Fuglestad, B.; Gupta, K.; Wand, A. J.; Sharp, K. A. Water Loading Driven Size, Shape, and Composition of Cetyltrimethylammonium/Hexanol/Pentane Reverse Micelles. *J. Colloid Interface Sci.* **2019**, 540, 207–217.
- (20) Sheu, E. Y.; Chen, S. H.; Huang, J. S. Structure and Growth of Bis(2-Ethylhexyl) Sulfosuccinate Micelles in Aqueous Solutions. *J. Phys. Chem. A* **1987**, *91*, 3306–3310.
- (21) Giordano, R.; Migliardo, P.; Wanderlingh, U.; Bardez, E.; Vasi, C. Structural Properties of Micellar Solutions. *J. Mol. Struct.* **1993**, 296. 265–269.
- (22) Gale, C. D.; Derakhshani-Molayousefi, M.; Levinger, N. E. How to Characterize Amorphous Shapes: The Tale of a Reverse Micelle. *J. Phys. Chem. B* **2022**, *126*, 953–963.
- (23) Baruah, B.; Crans, D. C.; Levinger, N. E. Simple Oxovanadates as Multiparameter Probes of Reverse Micelles. *Langmuir* **2007**, 23, 6510–6518.
- (24) Marques, B. S.; Nucci, N. V.; Dodevski, I.; Wang, K. W. C.; Athanasoula, E. A.; Jorge, C.; Wand, A. J. Measurement and Control of pH in the Aqueous Interior Micelles. *J. Phys. Chem. B* **2014**, *118*, 2020–2031.
- (25) Mukherjee, P.; Gupta, S.; Rafiq, S.; Yadav, R.; Jain, V. K.; Raval, J.; Sen, P. Ramping of pH across the Water-Pool of a Reverse Micelle. *Langmuir* **2016**, 32, 1693–1699.
- (26) Gębicki, J. L.; Szymańska-Owczarek, M.; Pacholczyk-Sienicka, B.; Jankowski, S. Ascorbyl Radical Disproportionation in Reverse Micellar Systems. *Radiat. Phys. Chem.* **2018**, *145*, 174–179.
- (27) Baruah, B.; Roden, J. M.; Sedgwick, M.; Correa, N. M.; Crans, D. C.; Levinger, N. E. When Is Water Not Water? Exploring Water Confined in Large Reverse Micelles Using a Highly Charged Inorganic Molecular Probe. J. Am. Chem. Soc. 2006, 128, 12758–12765.
- (28) Harris, R. K.; Mann, B. E. NMR and the Periodic Table; Academic Press, 1978.
- (29) Xu, Z.; Zhao, Y. ¹⁹F-Labeled Molecular Probes for NMR-Based Detection. *J. Fluorine Chem.* **2023**, 266, No. 110089.
- (30) Cametti, M.; Crousse, B.; Metrangolo, P.; Milani, R.; Resnati, G. The Fluorous Effect in Biomolecular Applications. *Chem. Soc. Rev.* **2012**, *41*, 31–42.
- (31) Barhate, N. B.; Barhate, R. N.; Cekan, P.; Drobny, G.; Sigurdsson, S. T. A Nonafluoro Nucleoside as a Sensitive ¹⁹F NMR Probe of Nucleic Acid Conformation. *Org. Lett.* **2008**, *10*, 2745–2747.
- (32) Dahanayake, J. N.; Kasireddy, C.; Karnes, J. P.; Verma, R.; Steinert, R. M.; Hildebrandt, D.; Hull, O. A.; Ellis, J. M.; Mitchell-Koch, K. R. Progress in Our Understanding of 19F Chemical Shifts. In

- Annual Reports on NMR Spectroscopy; Academic Press, 2018; Vol. 93, pp 281–365.
- (33) Gimenez, D.; Phelan, A.; Murphy, C. D.; Cobb, S. L. F-19 NMR as a Tool in Chemical Biology. *Beilstein J. Org. Chem.* **2021**, *17*, 293–318
- (34) Tong, J. P. K.; Langford, C. H.; Stengle, T. R. Nuclear Magnetic Resonance Studies of Solvation of Halides: ¹⁹F Studies of Solvent and Counterion Effects on Chemical Shift. *Can. J. Chem.* **1974**, *52*, 1721–1731.
- (35) Yu, J.-X.; Hallac, R. R.; Chiguru, S.; Mason, R. P. New Frontiers and Developing Applications in ¹⁹F NMR. *Prog. Nucl. Magn. Reson. Spectrosc.* **2013**, *70*, 25–49.
- (36) Kenwright, A. M.; Kuprov, I.; Luca, E. D.; Parker, D.; Pandya, S. U.; Senanayake, P. K.; Smith, D. G. ¹⁹F NMR Based pH Probes: Lanthanide(III) Complexes with PH-Sensitive Chemical Shifts. *Chem. Commun.* **2008**, 2514–2516.
- (37) Gerken, J. B. Measurement of pH by NMR Spectroscopy in Concentrated Aqueous Fluoride Buffers. *J. Fluorine Chem.* **2011**, *132*, 68–70.
- (38) Mehta, V. D.; Kulkarni, P. V.; Mason, R. P.; Constantinescu, A.; Aravind, S.; Goomer, N.; Antich, P. P. 6-Fluoropyridoxol: A Novel Probe of Cellular pH Using ¹⁹F NMR Spectroscopy. *FEBS Lett.* **1994**, 349, 234–238.
- (39) Connick, R. E.; Poulson, R. E. Electrolyte Effects on Nuclear Magnetic Resonance Frequencies of Fluorine in Aqueous Solutions. *J. Phys. Chem. A* **1958**, *62*, 1002–1004.
- (40) Sears, R. E. J. Fluorine Chemical Shifts in the Alkali Fluorides. *J. Chem. Phys.* **1974**, *61*, 4368–4369.
- (41) Stahla, M. L.; Baruah, B.; James, D. M.; Johnson, M. D.; Levinger, N. E.; Crans, D. C. ¹H NMR Studies of Aerosol-OT Reverse Micelles with Alkali and Magnesium Counterions: Preparation and Analysis of MAOTs. *Langmuir* **2008**, *24*, 6027–6035.
- (42) Glasoe, P. K.; Long, F. A. Use of Glass Electrodes to Measure Acidities in Deuterium Oxide. *J. Phys. Chem. A* **1960**, *64*, 188–190.
- (43) PubChem. Hydrofluoric acid, 2022 https://pubchem.ncbi.nlm.nih.gov/compound/14917.(accessed 2022-06-22).
- (44) Cai, S.-H.; Chen, Z.; Xu, X.; Wan, H.-L. Ab Initio Calculations of 19FNMR Chemical Shielding for Alkali-Metal Fluorides. *Chem. Phys. Lett.* **1999**, 302, 73–76.
- (45) Gerken, M.; Boatz, J. A.; Kornath, A.; Haiges, R.; Schneider, S.; Schroer, T.; Christe, K. O. The ¹⁹F NMR Shifts Are Not a Measure for the Nakedness of the Fluoride Anion. *J. Fluorine Chem.* **2002**, *116*, 49–58.
- (46) Malinowski, E. R.; Knapp, P. S.; Feuer, B. NMR Studies of Aqueous Electrolyte Solutions. I. Hydration Number of NaCl Determined from Temperature Effects on Proton Shift. *J. Chem. Phys.* **1966**, *45*, 4274–4279.
- (47) Fathi, H.; Kelly, J. P.; Vasquez, V. R.; Graeve, O. A. Ionic Concentration Effects on Reverse Micelle Size and Stability: Implications for the Synthesis of Nanoparticles. *Langmuir* **2012**, *28*, 9267–9274.
- (48) Ridley, R. E.; Fathi-Kelly, H.; Kelly, J. P.; Vasquez, V. R.; Graeve, O. A. Predicting the Size of Salt-Containing Aqueous Na-AOT Reverse Micellar Water-in-Oil Microemulsions with Consideration for Specific Ion Effects. *J. Colloid Interface Sci.* **2021**, 586, 830–835.
- (49) Ridley, R. E.; Fathi-Kelly, H.; Kelly, J. P.; Vasquez, V. R.; Graeve, O. A. Predicting Destabilization in Salt-Containing Aqueous Reverse Micellar Colloidal Systems. *ACS Earth Space Chem.* **2021**, *5*, 2223–2232.
- (50) Fifen, J. J.; Agmon, N. Ionic Radii of Hydrated Sodium Cation from QTAIM. *J. Chem. Phys.* **2019**, *150*, No. 034304.
- (51) Smith, A. M.; Lee, A. A.; Perkin, S. The Electrostatic Screening Length in Concentrated Electrolytes Increases with Concentration. *J. Phys. Chem. Lett.* **2016**. *7*. 2157–2163.
- (52) Gebbie, M. A.; Dobbs, H. A.; Valtiner, M.; Israelachvili, J. N. Long-Range Electrostatic Screening in Ionic Liquids. *Proc. Natl. Acad. Sci. U.S.A.* **2015**, *112*, 7432–7437.

- (53) Wiebenga-Sanford, B. P.; DiVerdi, J.; Rithner, C. D.; Levinger, N. E. Nanoconfinement's Dramatic Impact on Proton Exchange between Glucose and Water. *J. Phys. Chem. Lett.* **2016**, *7*, 4597–4601.
- (54) Bodor, A.; Tóth, I.; Bányai, I.; Szabó, Z.; Hefter, G. T. ¹⁹F NMR Study of the Equilibria and Dynamics of the Al³⁺/F⁻ System. *Inorg. Chem.* **2000**, *39*, 2530–2537.
- (55) Finney, W. F.; Wilson, E.; Callender, A.; Morris, M. D.; Beck, L. W. Reexamination of Hexafluorosilicate Hydrolysis by ¹⁹F NMR and pH Measurement. *Environ. Sci. Technol.* **2006**, *40*, 2572–2577.
- (56) Falcone, R. D.; Correa, N. M.; Biasutti, M. A.; Silber, J. J. Acid-Base and Aggregation Processes of Acridine Orange Base in n-Heptane/AOT/Water Reverse Micelles. *Langmuir* **2002**, *18*, 2039–2047.
- (57) Fujii, H.; Kawai, T.; Nishikawa, H. Determination of pH in Reversed Micelles. Bull. Chem. Soc. Jpn. 1979, 52, 2051–2055.
- (58) Halliday, N. A.; Peet, A. C.; Britton, M. M. Detection of pH in Microemulsions, without a Probe Molecule, Using Magnetic Resonance. *J. Phys. Chem. B* **2010**, *114*, 13745–13751.
- (59) Karpe, P.; Ruckenstein, E. Effect of Hydration Ratio on the Degree of Counterion Binding and pH Distribution in Reverse Micelles with Aqueous Core. *J. Colloid Interface Sci.* **1990**, 137, 408–424.
- (60) Muñoz-Santiburcio, D.; Wittekindt, C.; Marx, D. Nanoconfinement Effects on Hydrated Excess Protons in Layered Materials. *Nat. Commun.* **2013**, *4*, No. 2349.
- (61) Oshitani, J.; Takashina, S.; Yoshida, M.; Gotoh, K. Water Pool pH of AOT-Based W/O Microemulsions at Various Water Contents Estimated by Absorbance Ratio of Pyranine. *J. Chem. Eng. Jpn.* **2008**, 41, 507–512.
- (62) Takagi, H.; Swaddle, T. The Aqueous Hexacyanoferrate(II/III) Self-Exchange Reaction at High-Pressures. *Inorg. Chem.* **1992**, 31, 4669–4673.
- (63) Dunbar, K.; Heintz, R. Chemistry of Transition Metal Cyanide Compounds: Modern Perspectives. *Prog. Inorg. Chem.* **1997**, 45, 283–391.
- (64) Crans, D. C. Aqueous Chemistry of Labile Oxovanadates: Relevance to Biological Studies. *Comments Inorg. Chem.* **1994**, *16*, 1–33.
- (65) Casado, A. L.; Espinet, P.; Gallego, A. M. Mechanism of the Stille Reaction. 2. Couplings of Aryl Triflates with Vinyltributyltin. Observation of Intermediates. A More Comprehensive Scheme. *J. Am. Chem. Soc.* **2000**, *122*, 11771–11782.
- (66) Rouzina, I.; Bloomfield, V. A. Force-Induced Melting of the DNA Double Helix. 2. Effect of Solution Conditions. *Biophys. J.* **2001**, 80, 894–900.
- (67) Nobrega, J. A.; Rocha, F. R. P. Ionic Strength Effect on the Rate of Reduction of Hexacyanoferrate(III) by Ascorbic Acid: A Flow Injection Kinetic Experiment. *J. Chem. Educ.* **1997**, *74*, No. 560.
- (68) Lawal, O. S. Functionality of African Locust Bean (Parkia Biglobossa) Protein Isolate: Effects of pH, Ionic Strength and Various Protein Concentrations. *Food Chem.* **2004**, *86*, 345–355.
- (69) Solomon, T. The Definition and Unit of Ionic Strength. J. Chem. Educ. 2001, 78, 1691–1692.
- (70) de Vicente, M. E. S. The Concept of Ionic Strength Eighty Years after Its Introduction in Chemistry. *J. Chem. Educ.* **2004**, *81*, 750–753.
- (71) Cai, S. H.; Chen, Z.; Wan, H. L. Theoretical Investigation of F-19 NMR Chemical Shielding of Alkaline-Earth-Metal and Alkali-Metal Fluorides. *J. Phys. Chem. A* **2002**, *106*, 1060–1066.
- (72) Deverell, C.; Schaumburg, K.; Bernstein, H. J. ¹⁹F Nuclear Magnetic Resonance Chemical Shift of Alkali Fluorides in Light- and Heavy-Water Solutions. *J. Chem. Phys.* **1968**, *49*, 1276–1283.
- (73) Christe, K. O.; Wilson, W. W. Nuclear Magnetic Resonance Spectrum of the Fluoride Anion. *J. Fluorine Chem.* **1990**, *46*, 339–342.